



HAL
open science

Photoinitiators Derived From Natural Product Scaffolds: Mono-Chalcones in Three-Component Photoinitiating Systems and their Applications in 3D Printing

Jacques Lalevee, Hong Chen, Guillaume Noirbent, Ke Sun, Damien Brunel,
Didier Gigmes, Fabrice Morlet-Savary, Yijun Zhang, Shaohui Liu, Pu Xiao, et
al.

► To cite this version:

Jacques Lalevee, Hong Chen, Guillaume Noirbent, Ke Sun, Damien Brunel, et al.. Photoinitiators Derived From Natural Product Scaffolds: Mono-Chalcones in Three-Component Photoinitiating Systems and their Applications in 3D Printing. *Polymer Chemistry*, 2020, 11 (28), pp.4647-4659. 10.1039/D0PY00568A . hal-02906501

HAL Id: hal-02906501

<https://hal.science/hal-02906501>

Submitted on 24 Jul 2020

HAL is a multi-disciplinary open access archive for the deposit and dissemination of scientific research documents, whether they are published or not. The documents may come from teaching and research institutions in France or abroad, or from public or private research centers.

L'archive ouverte pluridisciplinaire **HAL**, est destinée au dépôt et à la diffusion de documents scientifiques de niveau recherche, publiés ou non, émanant des établissements d'enseignement et de recherche français ou étrangers, des laboratoires publics ou privés.

Photoinitiators Derived From Natural Product Scaffolds: Mono-Chalcones in Three-Component Photoinitiating Systems and their Applications in 3D Printing

Hong Chen¹, Guillaume Noirbent², Ke Sun¹, Damien Brunel², Didier Gimes², Fabrice Morlet-Savary¹, Yijun Zhang¹, Shaohui Liu¹, Pu Xiao^{3*}, Frédéric Dumur^{2*}, Jacques Lalevée^{1*}

¹ Institut de Science des Matériaux de Mulhouse, IS2M-UMR CNRS 7361, UHA, 15, rue Jean Starcky, Cedex 68057 Mulhouse, France

² Aix Marseille Univ, CNRS, ICR UMR 7273, F-13397 Marseille, France

³ Research School of Chemistry, Australian National University, Canberra, ACT 2601, Australia

* Corresponding author: jacques.lalevee@uha.fr (J. L.), frederic.dumur@univ-amu.fr (F.D.); pu.xiao@anu.edu.au (P. X.); Tel.: +33-(0)3-8960-8803 (J. L.); +33-(0)4-9128-9059 (F. D.).

Abstract: The design and development of high-performance photoinitiating systems applicable to visible light delivered from light-emitting diodes (LEDs) attracts an ever-increasing attention due to their great potential applications in various fields. Chalcones correspond to a well-established class of natural compounds present in many plants. In this context, photoinitiators based on the scaffolds of natural compounds have probably a great potential to open the way for non-toxic photoinitiators in the manufacture of biocompatible polymer materials. **In this work, 23 different chalcones selected from in-silico molecular design (i.e. through molecular orbital calculations) are used** in conjunction with an amine i.e. ethyl 4-(dimethylamino) benzoate (EDB) and an iodonium salt (*bis*-(4-*tert*-butylphenyl)iodonium hexafluorophosphate, Iod) to form photoinitiating systems (PISs) capable to initiate the polymerization of polyethylene glycol (600) diacrylate (PEG-diacrylate) via an oxidation–reduction reaction mechanism. The formation of hydrogels by photopolymerization of PEG-acrylate is found very efficient. Remarkably, 10 of the 23 Chalcones are completely new and even never synthesized prior to this work (Chalcone 4, 5, 7, 8, 9, 10, 12, 15, 16 and 21). By using computational quantum chemistry, fluorescence, steady-state photolysis, and electron spin resonance spin-trapping techniques, the photoinitiation mechanism of three-component photoinitiating systems based on chalcones/Iod/EDB are clarified. The results demonstrate that several chalcones-based PISs can initiate the free radical photopolymerization. Moreover, the developed chalcone-based three-component systems are applied to generate 3D hydrogel patterns using the 3D laser write technology. This research represents some novel insights into photopolymerization reactions with three-component photoinitiating systems used for 3D printing of hydrogels.

Keywords: chalcone; Claisen Schmidt condensation, free radical polymerization; three-component photoinitiating system; 3D printing.

1. Introduction

Since the early 1970s, the free radical photopolymerization has been extensively studied, as this polymerization technique is likely to provide a useful method for generating polymers suitable for various applications ranging from imaging, radiation curing, and optics technologies to (bio)medicine, microelectronics, and material science, while using a traceless reagent to activate the polymerization process, namely light [1-6]. An efficient photoinitiator (PI), which absorbs a certain wavelength of light to generate an active species (e.g., cation or free radical), is an essential component in the photopolymerization process [7-10]. **Although, several metal complexes or metal based compounds (e.g. ruthenium, copper, iron or iridium complexes) have been introduced into the photoinitiating systems in the polymer photochemistry field at room temperature under visible light, Acylgermanes (ketones**

containing germanium) were also proposed as visible light sensitive photoinitiators due to a significant red-shift of the $n-\pi^*$ transition; furthermore, it can produce free radicals upon light irradiation through α -cleavage process to initiate the FRP of (meth)acrylate or the CP of EPOX in combination with iodonium salt [8]. However, finding a new high-performance photoinitiation system in order to make the photopolymerization process more efficient upon irradiation with a visible light source is still one of the crucial aspects for the development of free radical photopolymerization reactions.

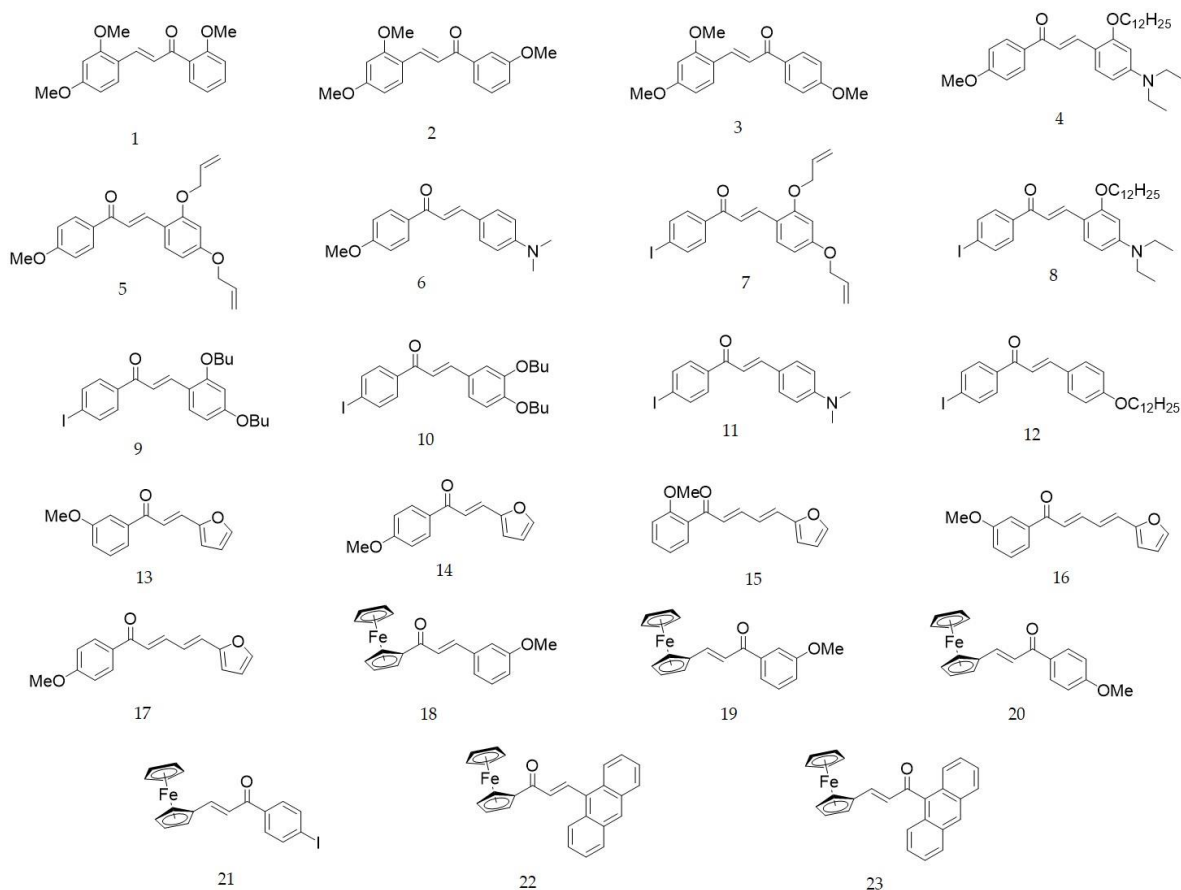
Plenty of studies have shown that some natural dyes have a great potential and can be used as non-toxic photoinitiators in the manufacture of biocompatible polymer materials [11-13]. After absorbing the appropriate light, natural dyes were promoted to an excited state, which can then interact with additives through an electron (or energy) transfer reaction to produce active species (e.g., a cation or a free radical) capable to initiate a photopolymerization reaction [14-16]. Reactivity between natural dyes and additives is closely related to their photochemical properties. In this context, chalcones are a well-established class of natural compounds present in many plants. Notably, chalcones which belong to flavonoids can be found in numerous edible plants such as fruits (tomatoes, apples, citrus), nuts and vegetables (potatoes, shallots, bean sprouts) so that their low environmental impact as well as their low toxicity for humans is thus averred.

Even if numerous investigations based on versatile photoinitiating systems were reported, **only very few chalcones have been reported by us to be activated in the visible light range and under low light intensity [17]. In this work, we want to extend this seminal work on the chalcone scaffold but using in-silico molecular design for the proposition and synthesis of new high performance structures. Indeed, these structures were first in-silico designed thanks to molecular modelling calculations to ensure good light absorption (particularly visible light) and high potential photoreactivity through high excited state energy. Remarkably, as a striking result of this in-silico design, 10 of the 23 proposed chalcones have never been reported in the literature and were specifically designed for this work, evidencing the novelty of the approach.**

Indeed, the elaboration of novel photoinitiating systems (PISs) suitable for irradiation at 405 nm are still actively researched. In order to initiate a free radical photopolymerization, novel photoinitiating systems comprising a chalcone with an attractive light absorption range as well as a chalcone exhibiting interesting photoinduced electron-transfer properties are proposed through the rational design of the molecular modeling [18-23]. On the basis of theoretical calculations aiming at optimizing the optical properties, the dyes proposed in this work are thus anticipated to exhibit the desirable properties that will allow these dyes to play a key-role in the proposed PISs. To evidence this, their polymerization efficiencies have been examined with benchmark monomers [e.g. polyethylene glycol (600) diacrylate, PEG-diacrylate] and this is the first time that such an approach and such a systematic study is carried out on a series of chalcone based photoinitiators.

In this paper, 23 different chalcones (Scheme 1) were designed and selected for their remarkable photophysical properties consisting in good near UV and visible light absorption properties which were predicted by molecular modeling design and synthesized directly from these theoretical data. Notably, a special focus has been devoted to developed chalcones substituted with a wide range of substituents including electron-donating groups (methoxy groups), heavy atoms (iodine), crosslinkable groups (allyloxy groups), redox active groups (ferrocene, pyrrole) or polyaromatic structures (anthracene). **Remarkably, 10 Chalcones proposed in this work were never synthesized before (Chalcone 4, 5, 7, 8, 9, 10, 12, 15, 16 and 21).**

Here, in the newly proposed three-component PISs, the chalcone derivatives, iodonium salt [*bis*-(4-*tert*-butylphenyl)-iodonium hexafluorophosphate, Iod; Speedcure 938], amine (ethyl dimethylaminobenzoate, EDB) were selected to act as photoinitiators, co-initiator and electron donor, respectively [24-27]. In addition, the visible light absorption properties, the photoinitiation abilities and the photochemical mechanisms of the proposed PISs at 405nm LED were characterized by time-resolved Fourier Transform InfraRed (FTIR) spectroscopy, UV-visible absorption and fluorescence spectroscopy as well as ESR experiments. To investigate the generation of free radicals and the excited state processes, the redox properties were also calculated and discussed. Finally, 3D printing experiments were carried out with the newly proposed three-component PISs, and excellent 3D patterns with excellent spatial resolution could be obtained.



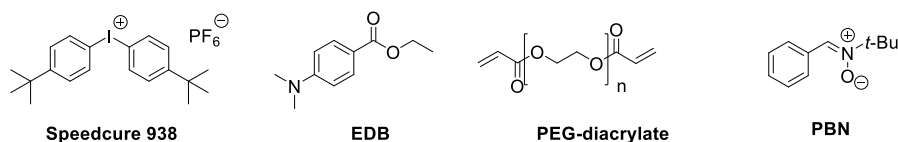
Scheme 1. The chemical structure of the chalcones 1-23 used in this study.

2. Experimental Part: Materials and Methods

2.1. Materials

The chalcones used as photoinitiators were prepared as reported in the supporting information and the chemical structures are depicted in the Scheme 1. The photopolymerizable monomer polyethylene glycol (600) diacrylate (PEG-acrylate: SR 610) was purchased from Sartomer-Europe, phenyl-*N*-*tert*-butylnitron (PBN), the solvent i.e. acetonitrile, the co-initiator (*bis*-(4-*tert*-butylphenyl)-iodonium hexafluorophosphate, Iod; Speedcure 938) and the electron donor (ethyl 4-(dimethylamino) benzoate, EDB; Speedcure EDB) were all purchased from Sigma-Aldrich, and their corresponding molecular structures are shown in the Scheme 2.

Scheme 2. The chemical structure of the iodonium salt (Speedcure 938), amine (Speedcure EDB), PBN and monomers used in this study.



2.2. Photopolymerization Reactions Monitored by Real Time Fourier Transformed Infrared Spectroscopy (RT-FTIR).

Briefly, the different chalcones 1-23, the iodonium salt, the amine EDB and the monomer (PEG-acrylate: SR 610 from Sartomer-Europe) were added into a small glass bottle, mixed well and finally stored in a dark environment before photo irradiation. In order to study the photopolymerization effect of the three-component photoinitiating systems, both photoinitiators (chalcones) and the additives, namely the iodonium salt (Speedcure 938) and the electron donor (Speedcure EDB) were weighted separately in order to respect the following conditions (chalcones/Iod/EDB :1.5%/1.5%/1.5% w/w/w), a typical formulation being prepared with 1 g of monomer and the different components introduced in weight percent according to the percentage mentioned above). The photopolymerization reactions were carried out between **two polypropylene films (thickness ~ 0.1 mm for thin films and ~1.8 mm for thick films)** under exposure to a visible LED emitting at 405 nm (the incidental light intensity I^0 at the samples surface was 110 mW.cm^{-2}). The polymerization process was carried out in laminated and at room temperature. As a control experiment, the monomer (1 g, PEG-acrylate) and only the additives i.e. the iodonium salt (Speedcure 938, 1.5%, w/w) and the electron donor (Speedcure EDB, 1.5%, w/w) were tested in the same conditions than that used for the three-component systems and used as the blank control. The conversion of the C=C double bond during the free radical photopolymerization process of the monomer (PEG-acrylate) was continuously monitored by Real Time Fourier Transform Infrared Spectroscopy (RT-FTIR, JASCO FTIR 4100) and focused on the vibration peak of acrylate C=C double bond between $\sim 1600 \text{ cm}^{-1}$ (thin films) or $\sim 16160 \text{ cm}^{-1}$ (thick films) versus irradiation time. The procedure used to monitor the photopolymerization profiles has already been described in detail in previous reports [28].

2.3. 3D patterning.

A computer programmed laser diode (Thorlabs) with a spot size of about 50 μm LED and a LED@405 nm as the light irradiation source was used to produce specific three-dimensional patterns from the developed three-component photoinitiator system with PEG-diacrylate. The compound was deposited into a homemade tank (2 mm thickness) and different laser speeds were investigated. Finally, the printed 3D patterns were observed through a numerical optical microscope (DSX-HRSU, OLYMPUS) [16].

2.4. UV-Visible Absorption Spectroscopy.

A JASCO V730 UV-visible spectrometer was used to study the absorption properties of the different compounds investigated in this work. The samples were analyzed in acetonitrile and the solutions were prepared so that the concentration was $5 \times 10^{-5} \text{ M}$. The LED@405 nm was selected as the light source for the photolysis experiments.

2.5. Electron Transfer Reaction for Chalcones Characterized by Fluorescence Experiments.

For the fluorescence properties, the chalcones were dissolved in acetonitrile and analyzed at a concentration of $1 \times 10^{-5} \text{ M}$ with a JASCO FP-6200 spectrofluorimeter.

2.6. Electron Spin Resonance Spin Trapping (ESR-ST).

Electron spin resonance (ESR) spin trapping experiments were carried out using an X-band spectrometer (Bruker EMXplus). The subsequent produced radicals were trapped in nitrogen saturated *tert*-butylbenzene solution at room temperature. A LED@405 nm was used as the light irradiation source and *N*-*tert*-Butyl- α -phenylnitron (PBN) as the spin trap agent. ESR spectra simulations were carried out using WINSIM software [29].

2.7. Swelling Kinetics

The swelling kinetics of polymerization products by the three-component photoinitiating systems based on chalcones/Iod/amine (1.5%/1.5%/1.5%, w/w/w) of PEG-diacrylate monomers were measured

by immersion in deionized water at room temperature. The products were then removed at various time points and the residual water at the surface of the products blotted with filter paper. Thereafter, the wet weight of each polymerization product was measured (Wt) and compared to the initial wet weight (Wo). The swelling ratio (Sr) was defined by equation 1 [30], as follows:

$$\text{Sr (\%)} = (\text{Wt}-\text{Wo})/\text{Wo} \times 100 \quad (1)$$

2.8. Molecular Modeling

Molecular Orbital calculations were performed by the Gaussian 03 suite of programs. Simulation of the UV absorption spectra and the triplet state energy levels for the chalcones were calculated with the time-dependent density functional theory at the MPW1PW91/6-31G* level of theory on the relaxed geometries calculated at the UB3LYP/6-31G* level of theory. The procedure is presented in [20-21].

3. Results

3.1 Photoinitiation Ability of the Chalcones Contained Three-Component Systems.

The photoinitiating abilities of all the three-component photoinitiating systems based on chalcones/Iod/amine (1.5%/1.5%/1.5%, w/w/w) were investigated with a PEG-diacrylate. The function conversion vs irradiation time profiles obtained using RT-FTIR are given in the Figure 1 and the final double bond conversions (FCs) of the monomer are summarized in the Table 1 (the FCs obtained using other chalcone-based PISs are summarized in Table S1). Compared to the blank control which only contains Iod and EDB (1.5%/1.5%, w/w, 49%), all the three-component systems showed better efficiencies to initiate the polymerization of thin samples in laminate upon irradiation with a LED@405 nm (Figure 1). For thick samples (1.8 mm), chalcone 12 exhibited a higher polymerization efficiency than the Iod/amine blank, evidencing the crucial role of chalcones on the polymerization initiating ability (Figure S1).

Figure 1c shows the polymerization profiles of the three-component systems based on chalcones bearing a furane group (chalcones 13-17). Although the FCs and polymerization rates were good in thin films, no cure in depth was observed in thick molds with these five chalcones. More interestingly, we observed that some photoinitiating systems based on the ferrocene-based mono-chalcones (chalcones 18-23) can initiate polymerization in thin films (Figure 1d). This is an interesting result as ferrocene derivatives are mainly used in literature to induce the polymerization of epoxy compounds [31-32]. Methoxy (1-6) or iodine (7-12) based chalcones (Figure 1a and 1b, respectively) show good efficiency with both high polymerization rates and FCs.

By comparing the polymerization efficiencies of the different samples, and more precisely, the final acrylate function conversions and polymerization rates, chalcones 4, 8, 9 and 10 proved to be excellent candidates to promote polymerization processes (e.g., the FCs of them were 89.9%, 79.3%, 84.6% and 81.8%, respectively). In addition, chalcone 12 proved to be the best candidate of the series since the polymerization of thick samples was possible with this dye (Figure S1). Therefore, chalcones 4, 8, 9, 10 and 12 were selected from the series of 23 chalcones as representative structures for more detailed investigations. Nevertheless, these chalcones all showed yellow fluorescence during the polymerization process. After polymerization, except for the polymerized product obtained with the chalcone 12, colors of the polymers obtained with all the other chalcones were deepened [33-34].

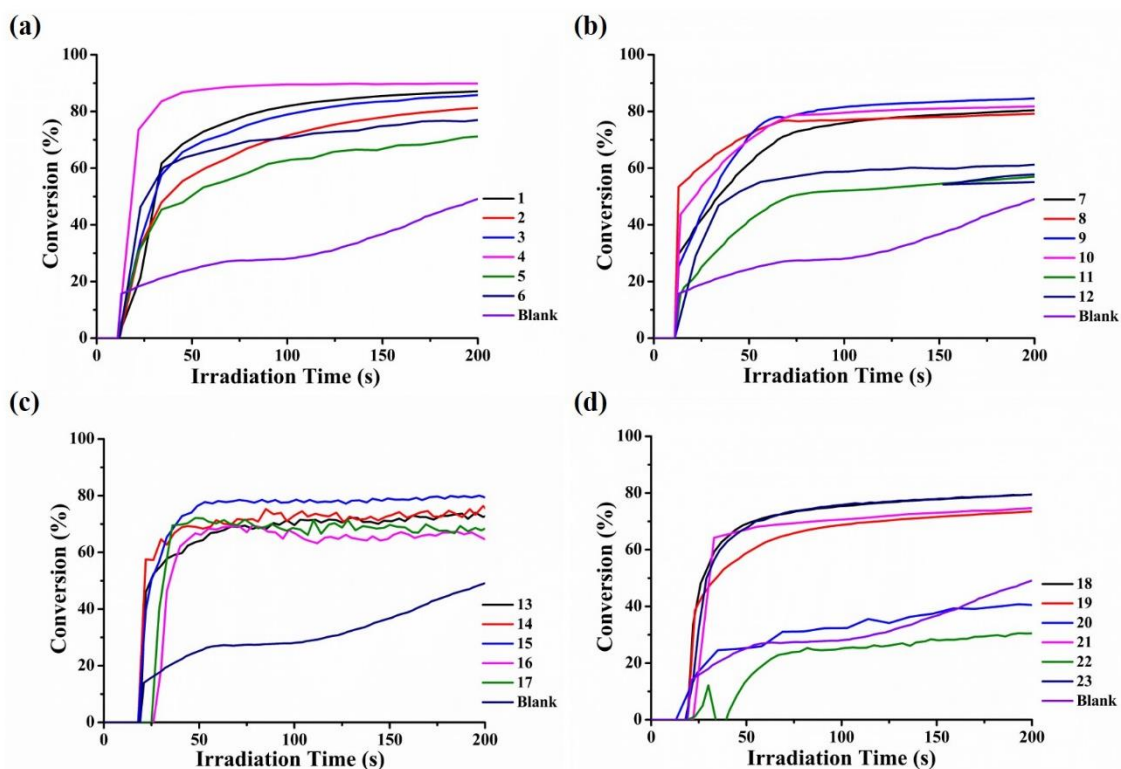


Figure 1. Photopolymerization profiles of PEG-diacrylate (conversions of C=C bonds vs irradiation time) initiated by iodonium salt (Speedcure 938) and amine (EDB) upon exposure to a LED@405 nm in laminate, at the same weight ratio chalcones 1-23: Iod: EDB = 1.5%:1.5%:1.5% in PEG-diacrylate, in the presence of (a) methoxy-based chalcones (chalcones 1-6); (b) iodine-based chalcones (chalcones 7-12); (c) furane-based chalcones (chalcones 13-17); (d) ferrocene-based chalcones (chalcones 18-23) in thin films; The irradiation starts for $t = 15$ s.

Table 1. Summary of the final acrylate function conversions (FCs) at 405 nm for the PEG-diacrylate monomer while using the three-component photopolymerization systems between chalcones (1.5%, w/w), iodonium salt (Speedcure 938, 1.5%, w/w) and amine (Speedcure EDB, 1.5%, w/w).

chalcone initiating systems in PEG-diacrylate						
Thin Films (~0.1 mm)	chalcone	4	8	9	10	Blank
	FC	89.9%	79.3%	84.6%	81.8%	49%
Thick Films (~1.8 mm)	chalcone	12	Blank			
	FC	90.9%	89.4%			

3.2 Formation of 3D patterns with Chalcones Contained Three-Component Photoinitiating Systems.

The free radical photopolymerization process of acrylates (PEG-diacrylate) could also be confirmed by the application in laser write experiments under air using the three-component photoinitiating systems based on chalcones/Iod/amine (1.5%/1.5%/1.5%, w/w/w). Tridimensional letter patterns “**CH E**” were fabricated from PEG-diacrylate initiated by the three-component photoinitiating systems based on the five selected reference chalcones (4, 8, 9, 10 and 12) upon irradiation at 405 nm with a laser. After that, a numerical optical microscope could be used to characterize the 3D patterns. As shown in Figure 2, the chalcone 12-based three-component photoinitiating system can easily write stable 3D PEG-based patterns with an excellent spatial resolution under a very short irradiation time due to its high photosensitivity. Contrarily to chalcone 12, chalcones 4, 9, 10 could still induce efficient

photopolymerization processes in the irradiated area but required longer irradiation time to produce 3D patterns (always with an excellent spatial resolution). Finally, chalcone 8 proved to be ineffective to form a complete and stable 3D product, irrespective of the irradiation time.

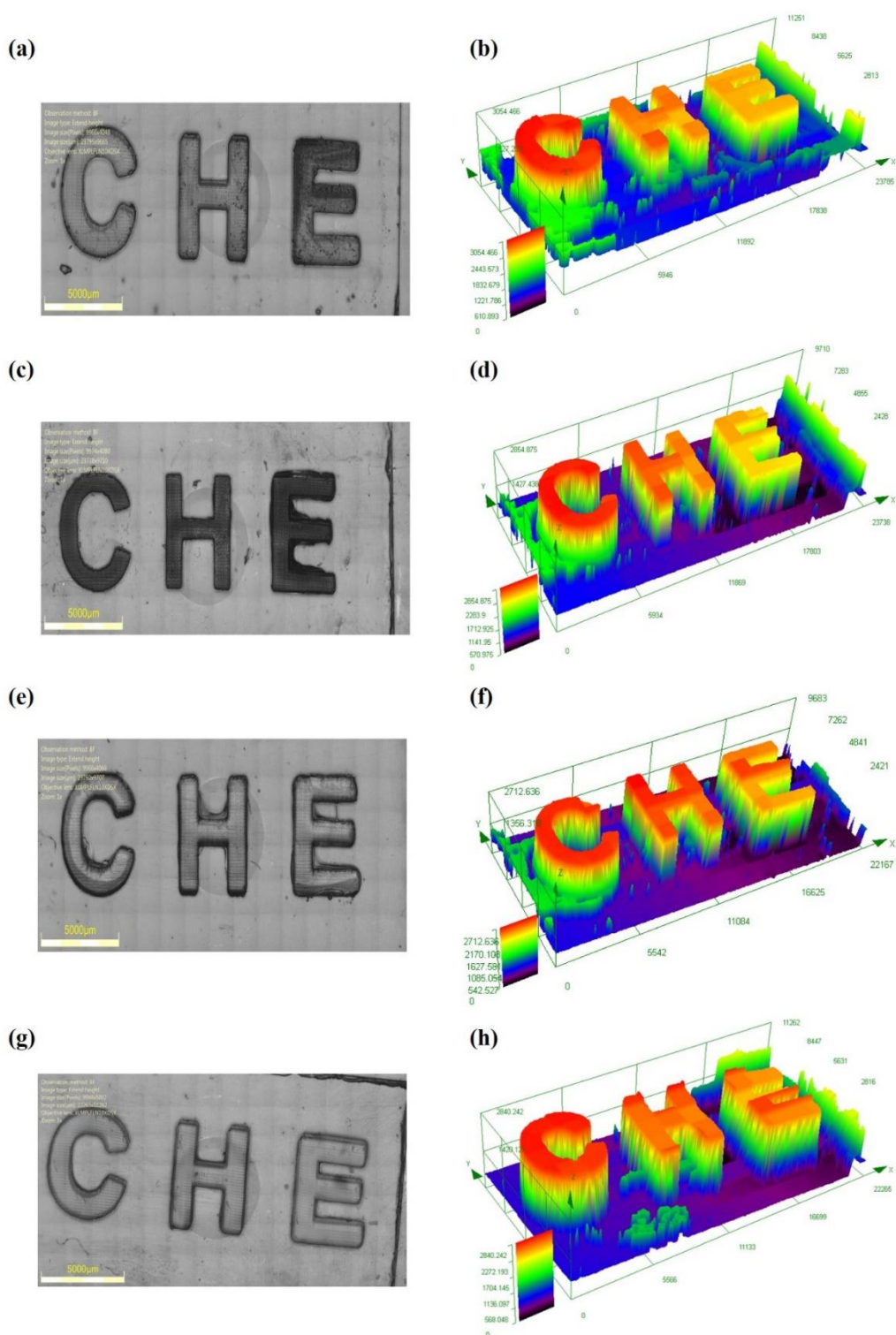


Figure 2. Free radical photopolymerization experiments for laser write initiated with chalcones based three-component photoinitiating systems using PEG-diacrylate as the monomer. Characterization of the 3D patterns by numerical optical microscopy: (left) top surface morphology (right) 3-D overall appearance of color pattern using chalcones/Iod/EDB (1.5%/1.5%/1.5%, w/w/w): (a) (b) chalcone 4; (c) (d) chalcone 9; (e) (f) chalcone 10; (g) (h) chalcone 12.

3.3 The Swelling Kinetics of PEG-Polymer Prepared Using Chalcones as Photoinitiators

The swelling kinetics of the PEG-polymers obtained using the three-component photoinitiating systems based on the chalcones were investigated by immersing the products in deionized water for 24 h. As shown in the Figure 3, the rate of swelling of the products gradually increased with time which reached a swelling equilibrium after 5 h. The best swelling ratio was obtained with chalcone 12 approaching 61%; for products based on the chalcone 4, the swelling ratio was about 55%. The preparation of hydrogels with the proposed photoinitiators is possible. These hydrogels can be prepared with a spatial control in 3D or laser write experiments (see 3.2).

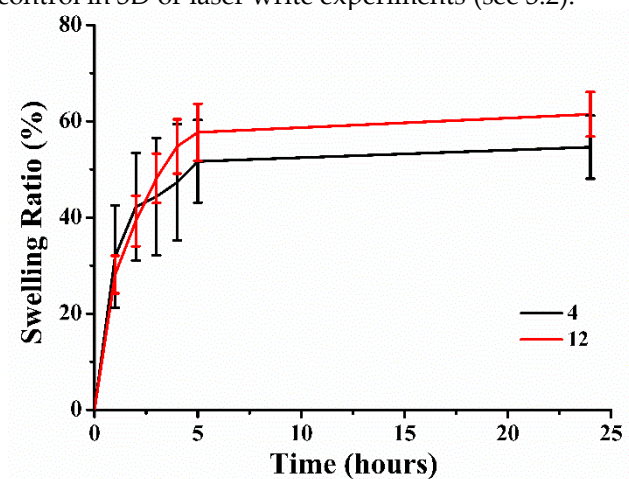


Figure 3. The swelling ratio of PEG-polymer prepared using chalcones 4 or 12 as photoinitiators (with Chalcone/Iod/amine: 1.5%/1.5%/1.5%, w/w/w).

4. Discussion

According to the results of FRP and 3D patterning experiments, the four selected chalcones (4, 9, 10 and 12) were chosen for the following mechanism studies.

4.1 Light Absorption Properties of the Chalcones in Acetonitrile

The UV-visible absorption spectra of chalcones (chalcones 4, 9, 10 and 12) in acetonitrile are presented in Figure 4, while their absorption maxima (λ_{\max}), extinction coefficients (ϵ_{\max}) at λ_{\max} and at the emission wavelength of the LED@405nm ($\epsilon_{@405\text{nm}}$) are listed in the Table 2. The maximum absorption of chalcones 4, 9, 10 and 12 appeared at 423 nm, 363 nm, 362 nm, and 344 nm, with the relevant extinction coefficients (ϵ_{\max}) of 21190 M⁻¹cm⁻¹, 15770 M⁻¹cm⁻¹, 18870 M⁻¹cm⁻¹ and 16950 M⁻¹cm⁻¹, respectively. The results indicate that the introduction of iodine could lead to strongly blue-shift transitions due to a minor resonance, and the lack of electron-donating ability of this group. The optimized geometries as well as the frontier orbitals (highest occupied molecular orbital [HOMO] and lowest unoccupied molecular orbital [LUMO]) are shown in Figure S2. Both the HOMOs and LUMOs were strongly delocalized all over the π -conjugated systems clearly showing the π - π^* transition as being the lowest energy transition [35-36].

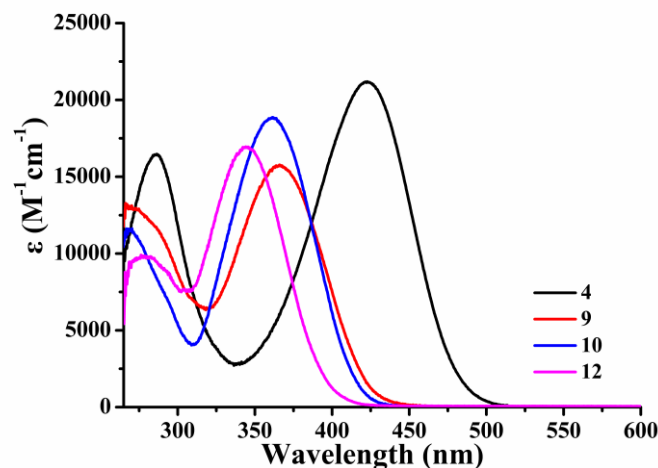


Figure 4. The UV-visible absorption spectra of chalcones 4, 9, 10 and 12 in acetonitrile.

Table 2. Light absorption properties of chalcones in acetonitrile: maximum absorption wavelengths λ_{\max} ; extinction coefficients at λ_{\max} (ϵ_{\max}) and extinction coefficients at the emission wavelength of the LED@405 nm ($\epsilon_{@405\text{nm}}$).

	λ_{\max} (nm)	ϵ_{\max} ($\text{M}^{-1}\text{cm}^{-1}$)	$\epsilon_{@405\text{nm}}$ ($\text{M}^{-1}\text{cm}^{-1}$)
chalcone 4	423	21190	18160
chalcone 9	363	15770	5800
chalcone 10	362	18870	4330
chalcone 12	344	16950	790

4.2 Steady State Photolysis of Chalcones 4, 9, 10 and 12 Characterized by UV-visible absorption Spectroscopy

The steady-state photolysis experiments done with the chalcones (e.g., chalcones 4, 9, 10 and 12) in the presence of the iodonium salt and the amine were carried out in acetonitrile upon irradiation with a LED@405 nm. The effect of the iodonium salt and the amine on the photolysis of the four chalcones are clearly shown in the Figure 5. Obvious and significant declines of the UV-visible absorption intensity were observed for the three-component photoinitiating systems based on the selected chalcones during light irradiation. Photolyses of chalcones 4, 9, 10 (the irradiation time \cong 10 s) were faster than that of the chalcone 12 (the irradiation time \cong 30 s) due to their higher molar extinction coefficients.

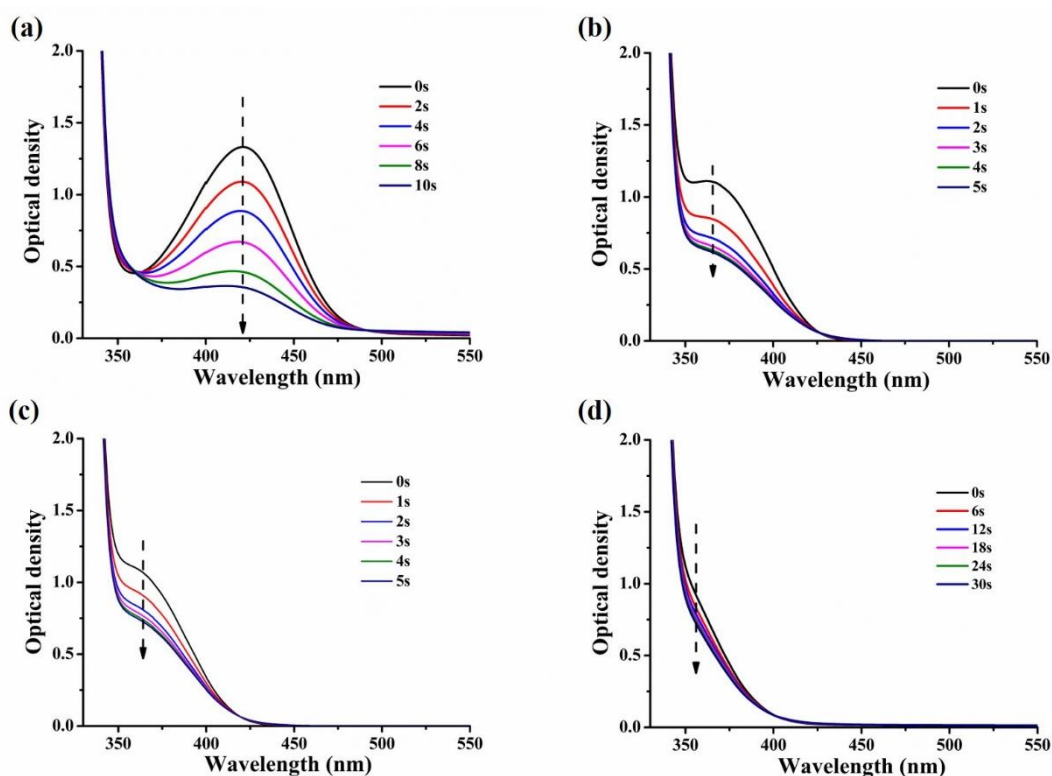


Figure 5. Photolysis of chalcones (5×10^{-5} M in acetonitrile) co-initiated with an iodonium salt (Speedcure 938, 0.01M) and an amine (Speedcure EDB, 0.01 M) upon exposure to LED@405nm under air in the solvent of acetonitrile: (a) chalcone 4; (b) chalcone 9; (c) chalcone10; (d) chalcone 12.

According to the proposed mechanism shown in Scheme 3, the reaction process can be divided in two parts: 1) the chalcones combined with the iodonium salt, and 2) the chalcones combined with the aromatic amine. UV-visible absorption spectra of the photolysis experiments done with the two two-component photoinitiating system (chalcones/Iod and chalcones/amine) are presented in the Figure 6 and Figure 7, respectively. In the presence of Iod (the same iodonium salt which is used in the three-component photoinitiating system), the absorption of the chalcones' characteristic peaks significantly decreased upon light irradiation (See Figure 6). Similarly, for the chalcones/amine systems (See Figure 7), significant changes could be detected within a few seconds on the absorption spectra of chalcones 4, 9 and 10 and these significant changes can be assigned to their high molar extinction coefficients at 405 nm (e.g. $\epsilon_{@405} = 18160 \text{ M}^{-1}\text{cm}^{-1}$ for chalcone 4, $\epsilon_{@405} = 5800 \text{ M}^{-1}\text{cm}^{-1}$ for chalcone 9 and $\epsilon_{@405} = 4330 \text{ M}^{-1}\text{cm}^{-1}$ for chalcone 10, respectively; see Table 2). Conversely, the photolysis process of chalcone 12 was very slow so that no significant change of the absorption under the same irradiation conditions could be observed.

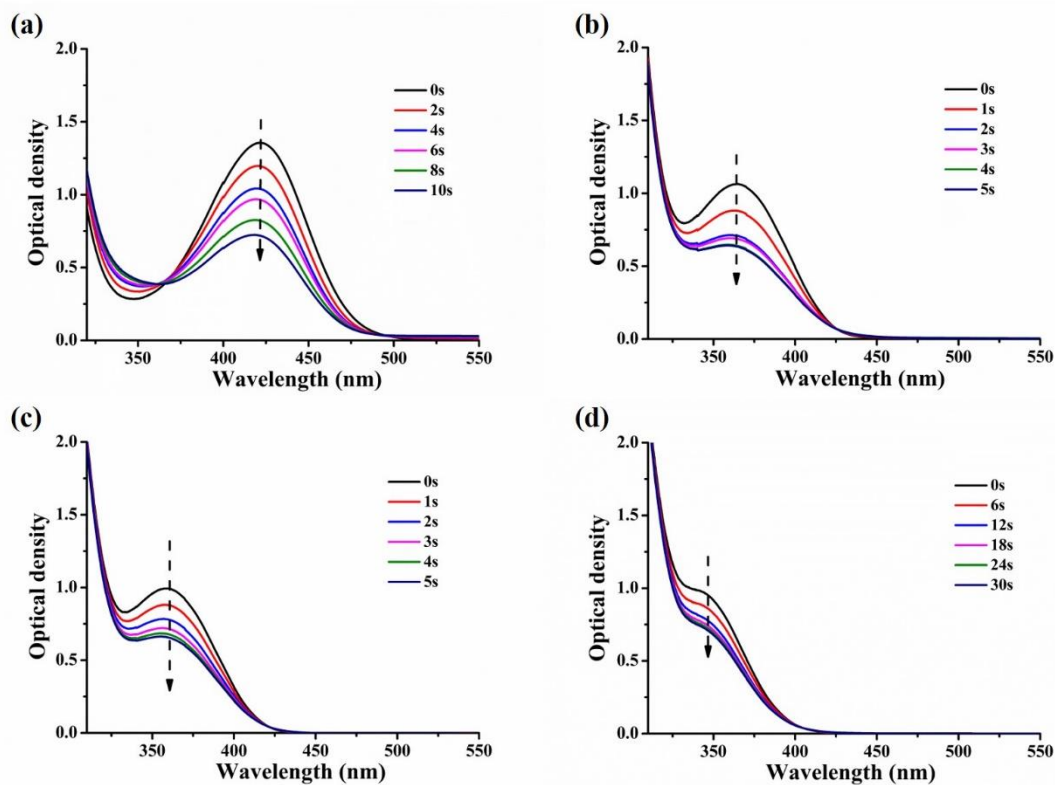


Figure 6. Photolysis of chalcones (5×10^{-5} M in acetonitrile) only in the presence of iodonium salt (Speedcure 938, 0.01M) upon exposure to LED@405nm under air in the solvent of acetonitrile: (a) chalcone 4; (b) chalcone 9; (c) chalcone 10; (d) chalcone 12.

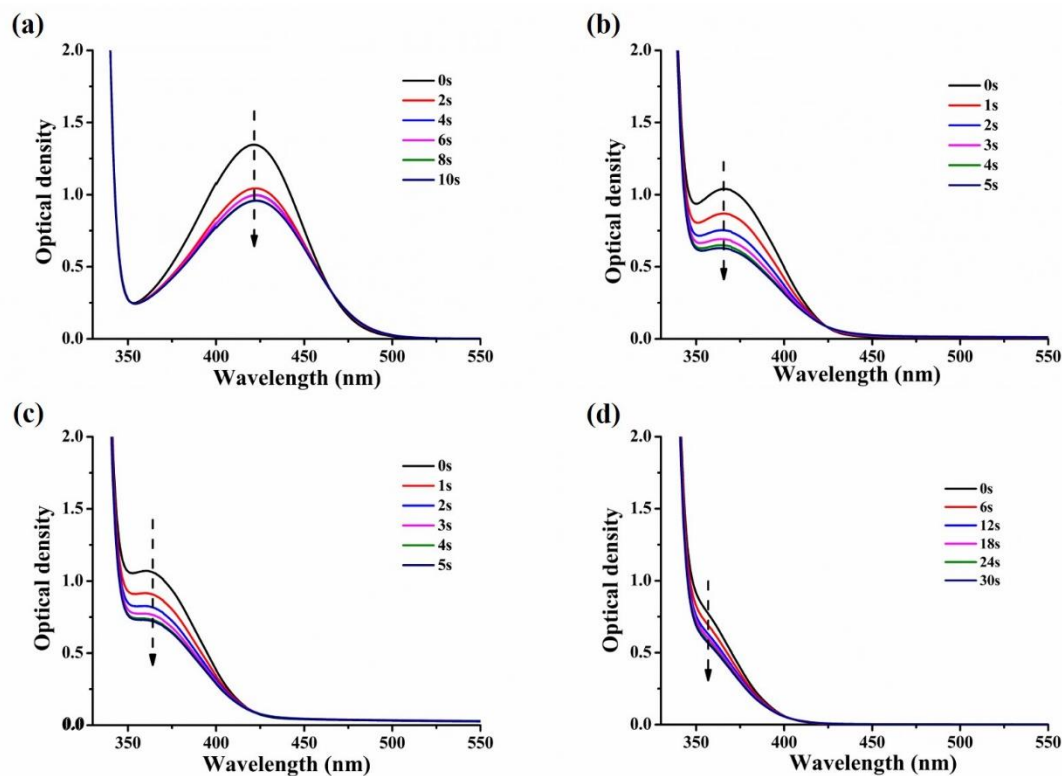


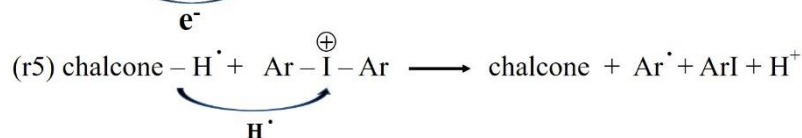
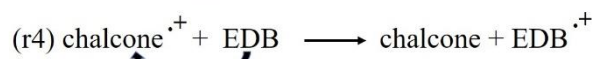
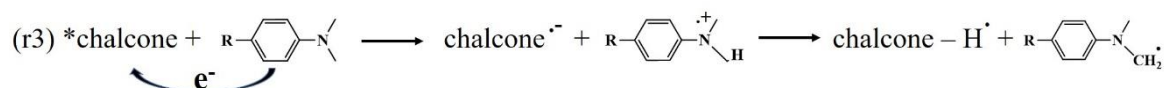
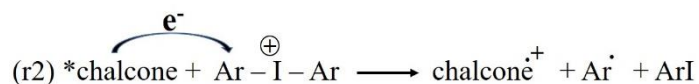
Figure 7. Photolysis of chalcones (5×10^{-5} M in acetonitrile) only in the presence of amine (EDB, 0.01 M) upon exposure to LED@405nm under air in the solvent of acetonitrile: (a) chalcone 4; (b) chalcone 9; (c) chalcone10; (d) chalcone 12.

4.3 Consumption of Chalcones in Photolysis Reactions

According to the UV-visible absorption spectra presented above, we can summarize the consumption of the chalcones vs. the irradiation time. Absorption changes detected in their UV-visible absorption spectra were examined both for the three-component PISs (chalcones/Iod/amine) and the two-component ones (chalcones/Iod or chalcones/amine) (Figure 8). For the three-component systems, we proposed that r1, r2 and r3 occurred. Reactions giving rise to the different radicals generated during photolysis are presented in the Scheme 3. It is obvious from the Figure 8a that the consumption of chalcone 4 achieved by the three-component PIS (chalcone 4/Iod/amine) was much higher than that observed for the two-component PIS based on chalcone 4/Iod and chalcone 4/amine combinations (e.g. the consumption of chalcone 4 = 71.0% for chalcone 4/Iod/amine vs 46.6% for chalcone 4/Iod or 28.7% for chalcone4/amine) which means that the interaction of three-component PIS based on chalcone 4 was more efficient than the two-component PIS.

As shown in the Figures 8b and 8c, for the same irradiation time, the consumption profile of chalcones 9 and 10 with the three-component PIS (chalcone 9/Iod/amine and chalcone 10 /Iod/amine) were quite close to that reached when using the two-component PISs based on chalcone 9/Iod and chalcone 10/Iod or chalcone 9/amine and chalcone 10/amine combinations (e.g. the consumption of chalcone 9 and 10 reached at 40%-45% and 30%-35%, respectively), which indicated that the interactions of the three-component PIS based on chalcones 9 and 10 are on par with those of the two-component PIS.

Interestingly, as shown in the Figure 8d, the chalcone 12/Iod combination could achieve the highest consumption of chalcone (~27.7%), while the chalcone 12/Iod/amine three-component system led to the lowest consumption (~17.6%). It is proposed that EDB^{•+} radical can be formed by electron transfer from EDB, as an *N*-aromatic electron donor to chalcones (r4), as well as chalcones can be regenerated from chalcone-H[•] in the presence of iodonium salt (r5), which decelerated the consumption of chalcone 12.



Scheme 3. Proposed photoinitiation mechanisms for the chalcones/Iod/amine redox combination.

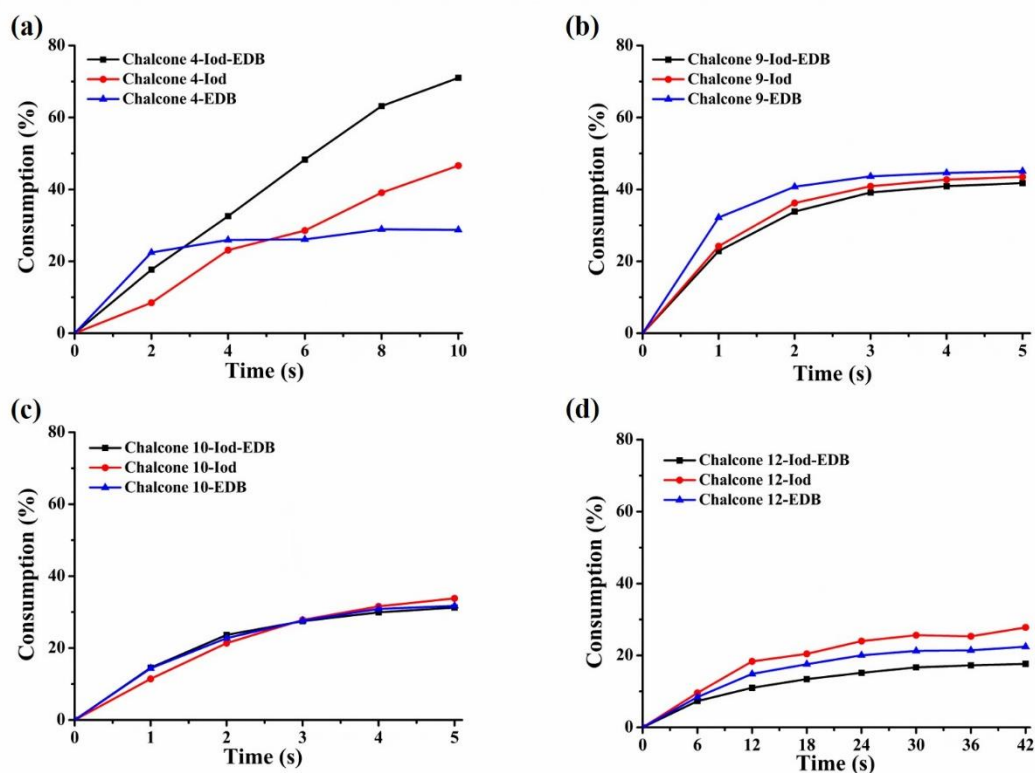


Figure 8. Consumption of (a) chalcone 4; (b) chalcone 9; (c) chalcone10; (d) chalcone 12 during the photolysis experiments

4.4 Fluorescence Quenching and ESR Experiments to Study Electron Transfer Reaction for Chalcones.

Fluorescence and UV-visible absorption spectra were measured in acetonitrile for chalcones 4, 9, 10 and 12 and the data are presented in the Figure 9. Actually, the first singlet excited state energy (E_{S1}) can be determined by the crossing point between the absorption of the UV-vis and the fluorescence spectra (e.g. $E_{S1} = 2.62$ eV for chalcone 4, 2.98 eV for chalcone 9, 2.92 eV for chalcone 10 and 3.15 eV for chalcone 12; Table 3).

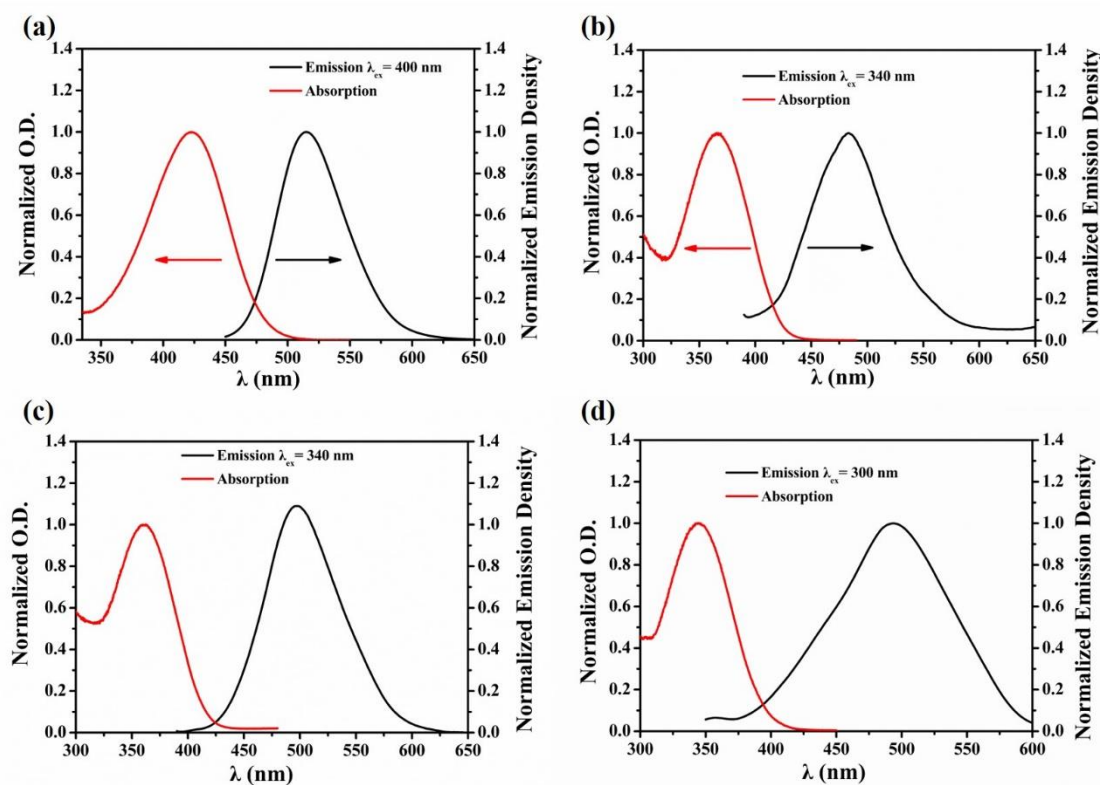


Figure 9. Singlet state energy determination in acetonitrile of (a) chalcone 4; (b) chalcone 9; (c) chalcone 10; (d) chalcone 12.

Fluorescence quenching experiments for chalcones 4, 9, 10 and 12 have been realized in acetonitrile to seek the theoretical feasibility of interactions between chalcone/Iod and chalcone/EDB. The results are presented in Figure 10 [37-38]. Fluorescence experiments of chalcone 4 showed a clear decrease of the fluorescence intensity as the quantity of the Iod salt or the amine increased in the solution, demonstrating that the addition of Iod or amine can interact with the chromophore in the excited singlet state. For chalcones 9 and 10, Iod salt also acted as a relatively good quencher, but with the amine added, the fluorescence intensity increased. More interestingly, there were no fluorescence quenching observed for the two-component systems chalcone 12/Iod and chalcone 12/amine and even, an increase of the fluorescence intensity was observed upon addition of Iod or amine, suggesting the formation of a complex. Interaction constant (K_{sv}) is obtained through Stern Volmer plot according to the well-known equation [37-38], then electron transfer quantum yields (Φ_{et} (Iod) and Φ_{et} (EDB)) for the according reactions (r2, r3) were calculated from equations 2 and 3 (Table 3).

$$\Phi_{et}^{Iod} = K^{sv}_{Iod} [Iod] / (1 + K^{sv}_{Iod} [Iod]) \quad (2)$$

$$\Phi_{et}^{EDB} = K^{sv}_{EDB} [EDB] / (1 + K^{sv}_{EDB} [EDB]) \quad (3)$$

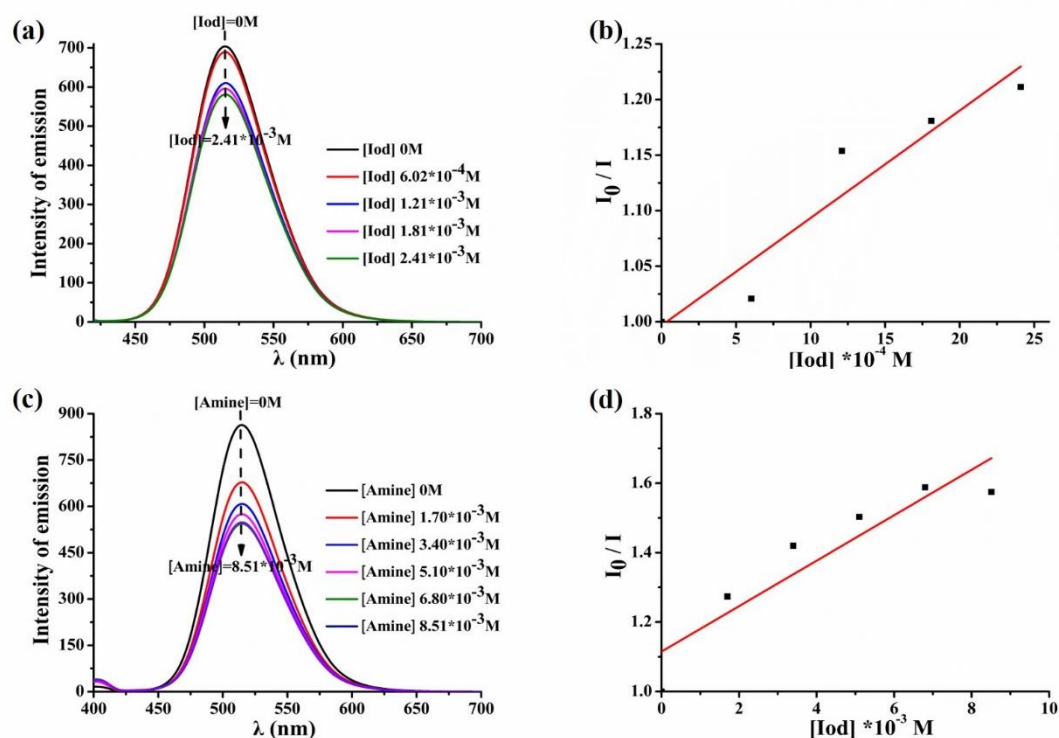


Figure 10. (a) Fluorescence quenching of chalcone 4 by the iodonium salt (Speedcure 938); (b) Stern-Volmer treatment for the chalcone 4/iodonium salt fluorescence quenching; (c) Fluorescence quenching of chalcone 4 by amine (EDB); (d) Stern-Volmer treatment for the chalcone 4/amine fluorescence quenching.

Table 3. Parameters characterizing the fluorescence properties of chalcone 4, 9, 10 and 12 in acetonitrile: Interaction constant (K_{sv}) between chalcone-Iod and chalcone-EDB systems calculated by Stern-Volmer equation; electron transfer quantum yield (Φ^{et}_{Iod}) of chalcone/Iod interaction and (Φ^{et}_{EDB}) of chalcone/EDB interaction.

	K_{sv}	Φ^{et}_{Iod}	K_{sv}	Φ^{et}_{EDB}	E_{s1} (eV)
chalcone 4	96.70	0.75	65.47	0.85	2.62
chalcone 9	66.28	0.67			2.98
chalcone 10	103.20	0.76			2.92
chalcone 12					3.15

Remarkably, very high electron transfer quantum yields (Φ^{et}) are calculated (Table 3) in agreement with efficient r2 and r3 processes. For Chalcone 12, the formation of a complex probably governs the reactivity of the system.

To better understand the interactions taking place in the three-component system chalcone/Iod/amine interaction, ESR-spin trapping experiments were carried out on chalcone/Iod, chalcone/amine solutions under N_2 in the presence of *N*-phenyl *tert*-butyl nitron (PBN) as the spin trap agent. As shown in the Figure 11, radical adducts were observed: hyperfine coupling constants for nitrogen and hydrogen of $a_N = 14.5$ G and $a_H = 2.2$ G were measured in the chalcone/Iod system; for the chalcone/amine system, the hyperfine coupling constants for nitrogen and hydrogen were characterized by $a_N = 14.4$ G and $a_H = 2.1$ G.

As reported in the literature, the PBN/aryl radical adduct is characterized by $a_N = 14.4$ and $a_H = 2.3$ G [39] which is presently in full agreement with r2 in the present ESR-ST experiments (Figure 11b). Concerning the chalcone/amine system the hyperfine coupling constants given by the simulated spectrum (Figure 11d) evidenced the generation of an aminoalkyl radical (r3) according to experimental data published elsewhere ($a_N = 14.4$ G and $a_H = 2.4$ G, [40]).

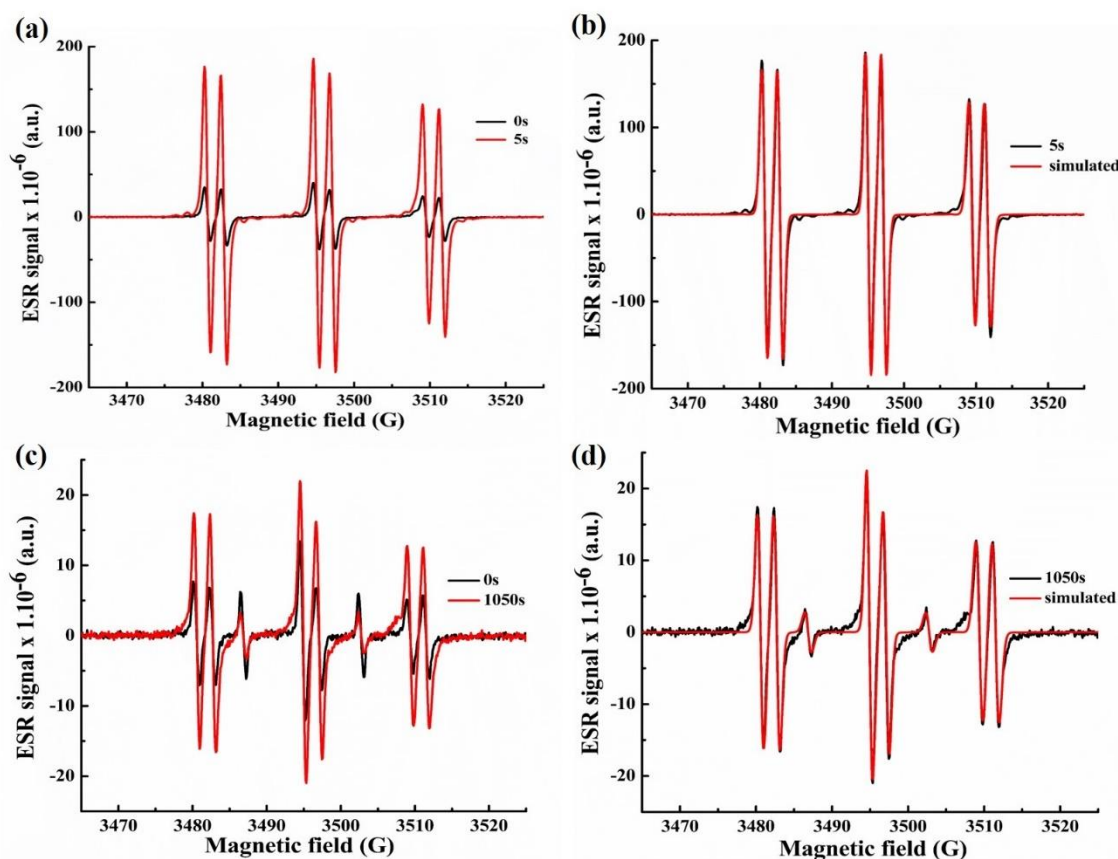


Figure 11. ESR spectra obtained from ESR-spin trapping experiment using PBN = 2 mg/mL (as spin trap agent); amine (Speedcure EDB) = 12.6 mg/mL; iodonium salt (Speedcure 938) = 12.6 mg/mL and chalcone 4 = 0.8 mg/mL in acetonitrile under N₂. (a), chalcone 4/Iod Irradiation time = 5 s (red) and = 0 s (black) spectra; (b) chalcone 4/Iod Irradiation time = 5 s (red) and simulated (black) spectra; (c) chalcone 4/EDB Irradiation time = 1050 s (red) and = 0 s (black) spectra (d) chalcone 4/EDB Irradiation time = 1050 s (red) and simulated (black) spectra.

5. Conclusions

In summary, the photoinitiation abilities of a series of three-component systems based on 23 different chalcones have been investigated using low intensity LED@405 nm as the light source. All chalcones exhibited a strong absorption in the visible light range and these structures proved to be very efficient for the free radical polymerization of acrylates under visible LEDs. Remarkably, chalcones 4, 9 and 10 were evaluated as reliable photoinitiators to promote efficient kinetics for the polymerization of PEG-diacrylate while using an iodonium salt (Speedcure 938) as the electron-acceptor and EDB as the electron-donor in thin film (thickness ~0.1 mm); in addition, chalcone 12 proved to be the best candidate to promote efficient kinetics for the polymerization of PEG-diacrylate under the same conditions in thick film (thickness ~1.8 mm). Radicals formed by the different photoinitiating systems have been characterized by Fluorescence quenching and ESR-spin trapping experiments. The high performance of chalcones in radical initiating systems were also shown through the 3D printing resins specially designed with the three-component photoinitiating systems previously studied. This work not only demonstrated the strong influence of the substitution pattern (*ortho*, *meta*, *para*-positions for the methoxy groups in chalcones 1-3), but also the choice of the different groups used to prepare chalcones (anthracene, ferrocene, alkoxy-substituted aromatic rings). With regards to the dramatic effect of the substitution on the photoinitiation abilities, no clear conclusions can be established at present, the best

chalcones 4, 9, 10 and 12 drastically differing in their structures. However, their light absorption properties and their ability to be involved in redox processes (with iodonium or amine) appear as key factor for good reactivity. Other deactivation pathway (back electron transfer reaction) must be also probably taken into account. Conscious of the influence of the substitution pattern as well as the selection of the functional groups used as substituents on chalcones, future prospects will thus consist in developing more extended families of chalcones to get a deeper insight into the exact role of these two parameters.

Supplementary Materials: The following are available online.

Acknowledgments: Authors wish to thank the Region Grand Est (France) for the grant “MIPPI-4D”. This research project is supported by China Scholarship Council (CSC) 201906280059. L’Agence de l’Innovation de Défense (AID) is acknowledged for its financial support through the PhD grant of Damien Brunel. This research was also funded by the Agence Nationale de la Recherche (ANR agency) through the PhD grant of Guillaume Noirbent (ANR-17-CE08-0054 VISICAT project). P. X. acknowledges funding from the Australian Research Council (FT170100301).

Conflicts of Interest: The authors declare no conflict of interest.

References

1. J. Ferraris, D.O. Cowan, V. Walataka Jr and J.H. Peristein, *J. Am. Chem. Soc.* 1973, **95**, 948.
2. K.D. Belfied and J.V. Crivello, (Eds.) *Photoinitiated Polymerization*; ACS Publications: Washington, DC, USA, 2003.
3. J. Zhang, N. Hill, J. Lalevee, J.P. Fouassier, J. Zhao, B. Graff, T.W. Schmidt, S.H. Kable, M.H. Stenzel, M.L. Coote and P. Xiao, *Macromol. Rapid. Commun.* 2018, **39**, e1800172.
4. H. Peng, S. Bi, M. Ni, X. Xie, Y. Liao, X. Zhou, Z. Xue, J. Zhu, Y. Wei, C.N. Bowman and Y.W. Mai, *J. Am. Chem. Soc.* 2014, **136**, 8855.
5. M. Sangermano, UV Cured nanostructured epoxy coatings. In *Epoxy Polymers New Materials and Innovations*; J.P. Pascault and R.J.J. Williams, Eds.; Wiley: Weinheim, Germany, 2010; pp. 235–249.
6. G. Gonzalez, A. Chiappone, I. Roppolo, E. Fantino, V. Bertana, F. Perrucci, L. Scaltrito, F. Pirri and M. Sangermano, *Polymer* 2017, **109**, 246–253.
7. M. Jin, M. Yu, Y. Zhang, D. Wan and H. Pu, *J. Polym. Sci., Part A: Polym. Chem.* 2016, **54**, 1945–1954.
8. P. Xiao, J. Zhang, F. Dumur, M.A. Tehfe, F. Morlet-Savary, B. Graff, D. Gigmes, J.P. Fouassier and J. Lalevée, *Prog. Polym. Sci.* 2015, **41**, 32–66.
9. J. Zhang, J. Lalevee, N.S. Hill, X. Peng, D. Zhu, J. Kiehl, F. Morlet-Savary, M.H. Stenzel, M.L. Coote and P. Xiao, *Macromol. Rapid. Commun.* 2019, **40**, e1900234.
10. J.P. Fouassier and J. Lalevée, *Photoinitiators for Polymer Synthesis-Scope, Reactivity, and Efficiency*; Wiley-VCH Verlag GmbH & Co. KGaA: Weinheim, Germany, 2012.
11. J.C. Zhao, J. Lalevee, H.X. Lu, R. MacQueen, S.H. Kable, T.W. Schmidt, M.H. Stenzel and P. Xiao, *Polym. Chem.* 2015, **6**, 5053.
12. J. Lalevée and J.P. Fouassier, *Dyes and Chromophores in Polymer Science*, ISTE Wiley, London 2015.
13. S. Telitel, S. Schweizer, F. Morlet-Savary, B. Graff, T. Tschanber, N. Blanchard, J.P. Fouassier, M. Lelli, E. Lacote and J. Lalevée, *Macromolecules* 2013, **46**, 43–48.
14. P. Xiao, J. Zhang, F. Dumur, M.A. Tehfe, F. Morlet-Savary, B. Graff, D. Gigmes, J.P. Fouassier and J. Lalevée, *Prog. Polym. Sci.* 2015, **41**, 32–66.
15. J. Radebner, A. Eibel, M. Leybold, C. Gorsche, L. Schuh, R. Fischer, A. Torvisco, D. Neshchadin, R. Geier, N. Moszner, R. Liska, G. Gescheidt, M. Haas and H. Stueger, *Angew. Chem. Int. Ed. Engl.* 2017, **56**, 3103–3107.
16. P. Xiao, F. Dumur, B. Graff, D. Gigmes, J.P. Fouassier and J. Lalevée, *Macromolecules*. 2014, **47**, 601–608.
17. M.A. Tehfe, F. Dumur, P. Xiao, M. Delgove, B. Graff, J.P. Fouassier, D. Gigmes and J. Lalevée. *Polym. Chem.* 2014, **5**, 382–390.
18. K. Sun, Y.Y. Xu, F. Dumur, F. Fabrice Morlet-Savary, H. Chen, C. Dietlin, B. Graff, J. Lalevée and P. Xiao, *Polym. Chem.* 2020, **11**, 2230–2242.
19. B. Beate Ganster, U.K. Fischer, N. Moszner and R. Liska, *Macromolecules* 2008, **41**, 2394–2400.
20. J. Zhang, F. Dumur, P. Xiao, B. Graff, D. Bardelang, D. Gigmes, J.P. Fouassier and J. Lalevée, *Macromolecules* 2015, **48**, 2054–2063.
21. N. Zivic, J. Zhang, D. Bardelang, F. Dumur, P. Xiao, T. Jet, D.L. Versace, C. Dietlin, F. Morlet-Savary, B. Graff, J.P. Fouassier, D. Gigmes and J. Lalevee *Polym. Chem.* 2016, **7**, 418–429.

22. N. Moszner, F. Zeuner, I. Lamparth and U.K. Fischer, *Macromol. Mater. Eng.* 2009, **294**, 877-886.
23. J.P. Fouassier, *Photoinitiation, photopolymerization, and photocuring: fundamentals and applications*. New York/Munich/Vienna: Hanser Publishers; 1995.
24. M. El-Roz, J. Lalevée, F. Morlet-Savary, X. Allonas and J.P. Fouassier, *Macromolecules* 2009, **42**, 4464-4469.
25. C. Dietlin, S. Schweizer, P. Xiao, J. Zhang, F. Morlet-Savary, B. Graff, J.P. Fouassier and J. Lalevée, *Polym. Chem.* 2015, **6**, 3895-3912.
26. O.I. Tarzi, X. Allonas, C. Ley and J.P. Fouassier, *J. Polym. Sci. Part A: Polym. Chem.* 2010, **48**, 2594-2603.
27. C. Grotzinger, D. Burget, P. Jacques and J.P. Fouassier, *Macromol. Chem. Phys.* 2001, **202**, 3513-3522.
28. J. Lalevée, N. Blanchard, M.A. Tehfe, F. Morlet-Savary and J.P. Fouassier, *Macromolecules* 2010, **43**, 10191-10195.
29. D.R. Duling, *J. Magn. Reson.* 1994, **104**, 105-110.
30. R. Holmes, X.B. Yang, A. Dunne, L. Florea, D. Wood and G. Tronci, *Polymer* 2017, **9**, 1-16.
31. B. Corakci, S.O. Hacioglu, L. Toppare and U. Bulut, *Polymer* 2013, **54**, 3182-3187.
32. J.A. Anderson, E. Hardgrove, T.B. Cavitt and P.C. Reeves, *J. Coat. Technol. Res.* 2007, **4**, 43-49.
33. J. Kabatc, *J. Photochem. Photobiol. A.* 2010, **240**, 1-11.
34. M.A. Tehfe, J. Lalevée, F. Fabrice Morlet-Savary, B. Graff, N. Blanchard and J.-P. Fouassier, *Macromolecules* 2012, **45**, 1746-1752.
35. M. Wakasa, K. Mochida, Y. Sakaguchi, J. Nakamura and H. Hayashi, *J. Phys. Chem.* 1991, **95**, 2241-2246.
36. M. Abdallah, D. Magaldi, A. Hijazi, B. Graff, F. Dumur, J.P. Fouassier, T.T. Bui, F. Goubard and J. Lalevée, *J. Polym. Sci. Part A: Polym. Chem.* 2019, **57**, 2081-2092.
37. D. Rehm, *Israel. J. Chem.* 1970, **8**, 259-271.
38. M. Atar, B. Öngel, H. Riedasch, T. Lippold, J. Neudörfl, D. Sampedro and A.G. Griesbeck, *Chem. Photo. Chem.* 2019, **1**, 89-97.
39. M.A. Tehfe, J. Lalevée, F. Morlet-Savary, B. Graff, N. Blanchard and J.P. Fouassier, *ACS. Macro. Lett.* 2012, **1**, 198-203.
40. J. Zhang, S.H. Wang, J. Lalevée, F. Morlet-Savary, E.S.H. Lam, B. Graff, J. Liu, F.Y. Xing and P. Xiao, *J. Polym. Sci.* 2020, **58**, 792-802.

TOC graphic:

